JOURNAL OF CATALYSIS 129, 414–425 (1991)

The Poisoning Action of Iron on Electrolytic Silver Catalysts Used for Partial Oxidation of Methanol

DENG JINGFA,* BAO XINHE,* AND DONG SHUZHONG†

*Chemistry Department, Fudan University, Shanghai 200433, People's Republic of China; and †Modern Physics Institute of Fudan University, Shanghai 200433, People's Republic of China

Received March 10, 1989; revised May 1, 1990

Poisoning of silver catalysts used for partial oxidation of methanol has been investigated by combined surface techniques including XPS, SIMS, SEM, TDS, TPRS, work function measurement, and microreactor studies. Results show that the oxidation path is governed mainly by surface iron loading. Once Fe_2O_3 is present at the catalyst surface, the catalytic performance degrades rapidly. The surface characteristics of iron depend strongly on the iron loading on the surface.
© 1991 Academic Press, Inc.

INTRODUCTION

Polycrystalline silver prepared by repetitive electrolytic refining is widely used as an industrial catalyst for the oxidation of methanol to formaldehyde (*1*). The process is carried out at a temperature above 900 K, using excess methanol relative to oxygen. It is possible to reach a selectivity of 90% at almost complete conversion (*2*). However, the iron which is sometimes present in the catalyst as a ferric oxide impurity, and in technical grade methanol as $Fe(CO)_5$, will cause degradation of the selectivity and result in more by-products, such as CO and CO_2 (*3*).

The deactivation effect was first reported in a review by Hughes (*4*). In some recent studies, Jede and Benninghoven investigated the poisoning action of iron on silver catalysts by using SIMS (*5*). It was suggested that the iron was adsorbed on the catalyst grains and acted as a poison mainly by changing the Ag–O bond energy (*6*). However, the surface structure of a poisoned catalyst has not been reported so far.

The oxidation mechanism of methanol to formaldehyde has been the subject of many studies. The following concepts are generally accepted (*7,8*):

(a) On a clean silver surface no adsorption of CH_3OH occurs; however, the surface preadsorbed oxygen can enhance both the adsorption and the oxidation of CH_3OH.

(b) The first step of the oxidation of CH_3OH is the dissociative adsorption of methanol over the oxygen preadsorbed on the surface to form surface methoxide and hydroxyl species, as was suggested in Barteau Madix's (*1*) work on Ag(110), as well as in our previous work on electrolytic silver by means of TPRS.

(c) The rate-determining step is the decomposition of surface methoxide species, and the activation energy for the process is about 24 kcal/mol.

Despite the progress indicated above, all the results obtained so far are for a pure Ag surface, and the mechanism of methanol oxidation on an iron-covered silver catalyst have not been reported. In our present studies the surface properties of the poisoned catalysts and the reaction behavior of methanol on iron-covered silver catalysts are investigated by combining catalysis research

0021-9517/91 $3.00
Copyright © 1991 by Academic Press, Inc.
All rights of reproduction in any form reserved.

and surface analysis with XPS, UPS, SIMS, TDS, TPRS, and the measurement of work function.

EXPERIMENTAL

1. Sample Preparation and Materials

The polycrystalline silver (purity 99.999%) was prepared by means of triple electrolytic refining. The preparation method as well as the surface structure of the electrolytic silver have been described elsewhere in detail (*8*). As in industrial catalysts, the particle size of the silver is about 100 μm in diameter, with a specific surface of 0.1 m^2g^{-1}, which does not change after catalytic reaction. The iron was introduced into the silver by chemical deposition from an aqueous solution of $Fe(NO_3)_3$ at a certain temperature, followed by calcination to 930 K for more than 3 h in air. The quantity of iron in the catalyst, which was determined by ICP–AES, was changed by controlling either the concentration of the $Fe(NO_3)_3$ solution or the deposition temperature. This iron-covered silver catalyst was used in studying catalytic activity.

For surface research, the samples were prepared by *in situ* gaseous deposition of $Fe(CO)_5$ on silver. Thus, the electrolytic silver powder was pressed into a disk of about 13 mm in diameter and fixed in a transferable sample holder. After the surface was cleaned by argon ion sputtering and checked by Auger electron spectroscopy (AES), the iron was introduced by *in situ* exposure of $Fe(CO)_5$ at room temperature, and then the sample was heated in oxygen atmosphere of about 10^{-7} Torr. When the sample was heated to 480 K, a large change in work function was measured, which indicted that both decomposition of $Fe(CO)_5$ and formation of iron oxide species had occurred. The coverage of iron was measured by AES. The oxidation state of iron was determined by XPS in a separate system, in which the samples were prepared by the same procedures.

High-purity CH_3OH (99.99%) was purchased from Shanghai Chemical Co. and further purified by prolonged pumping at about 120 K until a constant mass spectroscopy signal distribution was obtained. Deuterated methanol, CH_3OD(99 wt%), obtained from Merck Co. was similarly purified. $^{18}O_2$ (>99%) was purchased from Amersham Co. and used without further purification.

2. Apparatus and Procedures

Catalytic measurements were performed in a fixed-bed reactor as described elsewhere (*9*). The reactor, a quartz tube with an i.d. of 18 mm, was loaded with 2- to 3-g catalyst. Methanol was injected into an evaporator by a micropump to be mixed with air before entering the reactor. The liquid product was cooled rapidly to room temperature and samples were analyzed by chemical method. The quantities of by-product, i.e., CO, and CO_2 in the tail gas, were determined by a gas analyzer.

Surface analysis was carried out with VG ESCA LAb 5 electron energy spectrometer, which provides XPS, UPS, and SIMS. The X-ray source used was Mg$K\alpha$. The pressure in the testing chamber was maintained at about 10^{-8} Pa during the experiments (*8*). The binding energy was calculated by using E_b(Ag $3d_{5/2}$) = 368.0 eV as a standard. The surface composition of iron was calculated from the peak area of its XPS based on the method described previously (*10*).

Static temperature-programmed reaction spectroscopy (TPRS) and steady-state temperature-programmed reaction spectroscopy (SSTPRS) (*11*) were used. A typical procedure for static TPRS of methanol has been previously described (*8*). A dose of purified methanol was added to the iron-modified silver surface. After reaching the desired exposure, the variable leak valve was turned off, and the residual methanol in the gas phase was rapidly pumped off. The sample was then heated, and the distribution of the reaction products were simultaneously detected with a mass spectrometer. By SSTPRS, the dosage rate of each reactant was kept constant during testing. In order to minimize the overlap of various

product signals, deuterated methanol (CH_3OD) was individually monitored by recording the mass 33 signals and others were identified by recording the mass 30(CH_2O); 28(CO); 44(CO_2), etc. The results obtained were calibrated by the relative strength of the mass spectroscopy.

RESULTS AND DISCUSSIONS

1. Catalytic Measurements for Iron-Covered Silver Catalyst

The experimental conditions chosen for the catalytic measurement were: temperature, 900 K; inlet concentration of methanol ($[CH_3OH]_{in}$), 60 wt%; the molar ratio of oxygen to methanol, 0.41; and the space velocity (V_s), $5 \times 10^4\ h^{-1}$. The V_s is defined as the ratio of total volume flow rate (0°C, 1 atm) to volume of the catalyst bed. The conversion is defined by

$$Y = \{\{[CH_3OH]_{in} - [CH_3OH]_{out}\}/[CH_3OH]_{in}\} \times 100\%$$

and the selectivity (S) to formaldehyde is defined by

$$S = \{[CH_2O]_{out}/\{[CH_3OH]_{in} - [CH_3OH]_{out}\}\} \times 100\%.$$

Figure 1 gives plots of the change in yield and conversion vs the concentration of iron in bulk. In comparison with the unpoisoned catalyst, the yield of CH_2O decreases progressively with increasing iron concentration. Increasing the surface iron to 10^3 ppm leads to a rapid drop in the CH_2O yield. It can be seen from Fig. 2 when iron is present at higher concentration (>1000 ppm) that the combustion reaction dominates and CO_2 increases rapidly. These results imply that the reaction path is governed mainly by the iron loading in the catalyst, and the poisoning action of iron can be approximately divided into two regions with a borderline of 1000 ppm concentration of iron. The catalyst in which the iron concentration less than 1000 ppm is defined as a slightly poisoned catalyst and the catalyst in which the iron concentration is greater than 1000 ppm is defined as a seriously poisoned catalyst.

2. XPS and Work Function Measurements

Figures 3 and 4 are the Fe($2p_{3/2}$) and O($1s$) core spectra of the ferric oxides, respectively. Except for the very low concentration of iron (curve 1), Fe($2p_{3/2}$) spectra shows a clear double-peak structure. One peak centered in binding energy of 708.5 eV and the other is around 710.5 eV. The binding energies (E_b) of various ferric oxides, i.e., Fe(0), Fe(II), and Fe(III), show large and regular chemical shifts, and based on XPS spectra various species can be distinguished easily (*12*). By comparing the results in Figs. 3 and 4 with Wandelt's result (*13*) (see Table 1), it can be confirmed that the low binding energy state corresponds to Fe(II) cation and the high binding energy state to Fe(III) cation.

The results of XPS show that on the slightly poisoned surface the iron is present mainly in the form of FeO. The amount of Fe_2O_3 increases rapidly, however, with increasing iron concentration, and eventually the FeO peak becomes invisible. *In situ* Mössbauer measurements also confirm that when the concentration of iron is higher than 1000 ppm, α-Fe_2O_3 dominates in the catalysts (this result will be published separately).

The O($1s$) binding energy presented in Table 1 shows that the O($1s$) peaks of two samples (Fe_xO, $\alpha - Fe_2O_3$) appear at a constant energy of 530.3 eV. In our results, only curve 5 (2660 ppm Fe) has a peak at this binding energy, and the other peaks are shifted to higher energy with the decrease of iron load. The maximum shift is to more than 2 eV. These unexpected chemical shifts of O($1s$) imply a strong interaction between the lattice oxygen of ferric oxides with the silver substrate. In order to make sure of this effect, a measurement of the work function change has been carried out, and the results are shown in Fig. 5. At clean silver surfaces the value of the work function (ψ) is 4.50 eV,

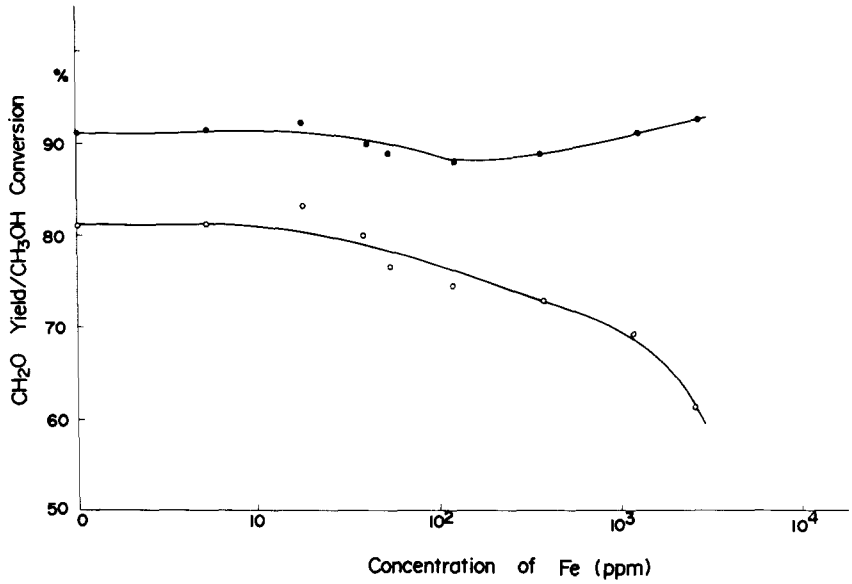

FIG. 1. The changes of selectivity (○) and conversion (●) for methanol oxidation to formaldehyde as a function of iron loads in silver catalysts. Reaction temperature, 900 K, the ratio of oxygen to methanol: 0.41.

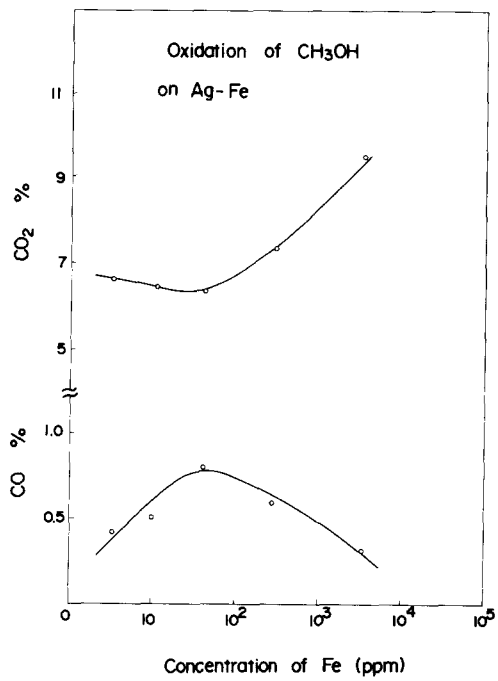

FIG. 2. Variation of CO and CO_2 vs the iron loads (ppm) in catalysts.

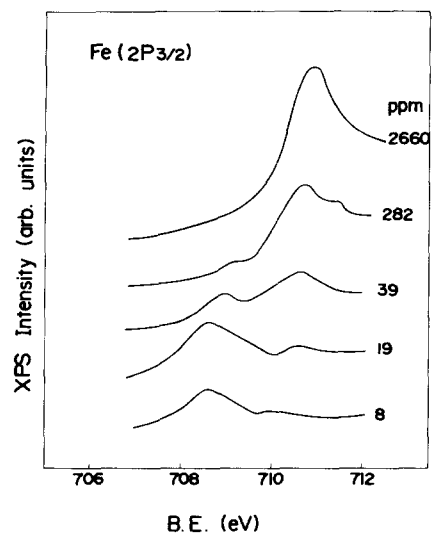

FIG. 3. X-ray photoelectron of the Fe($2p_{3/2}$) on various iron-loaded catalysts. Concentration of iron in bulk: (1) 8 ppm, (2) 19 ppm, (3) 39 ppm, (4) 282 ppm, (5) 2660 ppm.

TABLE 1

Comparison of XPS Core Level Data of Standard Iron Oxide and Ferric Oxides Loaded on Silver

Sample	Fe($2p_{3/2}$) E_b (eV)	FWHM (eV)	O($1s$) E_b (eV)
Fe Metal	707.0	2.0	—
Fe_xO	709.7	4.5	530.3 [13]
α-Fe_2O_3	711.2	4.5	530.3 [13]
Low iron surface	708.5	4.0	532.0 (This work)
High iron surface	710.5	4.0	530.0 (This work)

and with increasing iron loading, ψ increases rapidly. Having passed through a maximum, the work function decreases progressively with increasing iron loading and at about 1000 ppm it reaches the value for the Fe-free silver ($\Delta\phi = 0$). Further increasing the iron loading the work function shows no significant change. This means that on the surface of seriously poisoned catalysts the interactions of Fe_2O_3 with the Ag surface disappear, which is in agreement with the XPS results.

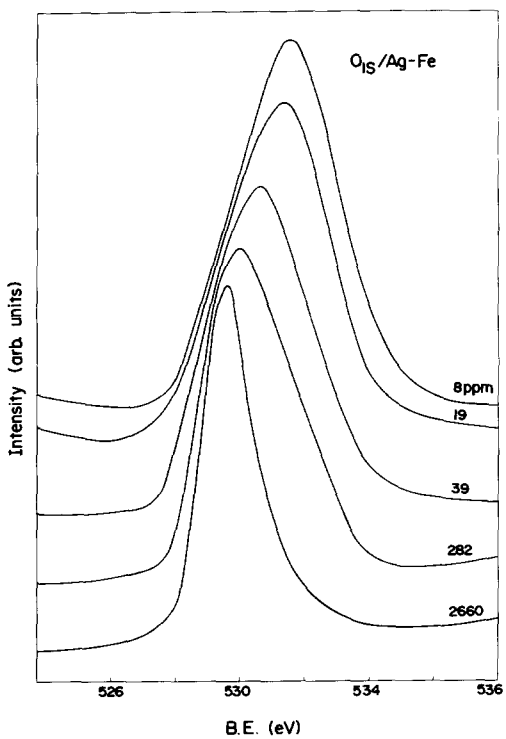

FIG. 4. X-ray photoelectron of O($1s$) on various iron-loaded catalysts. (1) 8 ppm, (2) 19 ppm, (3) 39 ppm, (4) 282 ppm, (5) 2660 ppm.

3. *SIMS and SEM Results*

The depth profile of iron in the silver substrate was observed by SIMS. In this analysis Ar^+ ion, having a primary energy of 5.5 keV, was used. The sputtering rate was about 5–10 Å/min and the analyzed area was 10^4 μm^2.

^{56}Fe intensity profiles for two different catalysts are shown in Fig. 6. The two samples show quite different features. For the low iron catalyst (10 ppm in bulk), the concentration of iron is of very large value at the surface and then drops rapidly. The region of high iron concentration is estimated to be less than 5 Å. For a high iron catalyst (1000 ppm in bulk), the iron signal decreases progressively and shows a moderate amount of iron to a depth of more than 50 Å. Our results of SIMS for the high-iron load catalyst can only be explained by the formation of iron islands or iron multilayers on the silver surface. In order to distinguish the two effects, the morphological configuration was investigated by a SEM. The micrograph for the high iron catalyst was shown in Fig. 7. It can be seen that disordered islands are present on this surface, and the size of the islands can be estimated roughly between 0.1 to 1 μm.

The results of SIMS confirm that on the low iron-loaded surface, iron is dispersed in

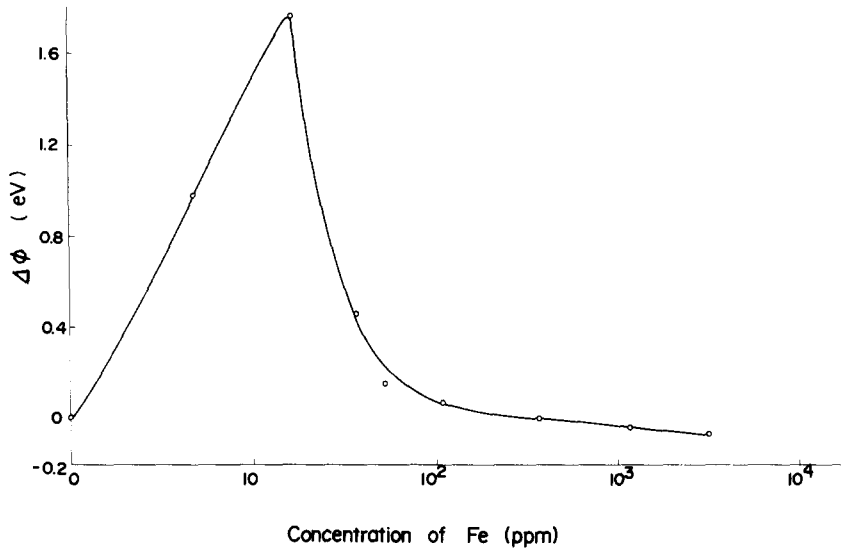

FIG. 5. Variation of work function change vs iron loads in catalysts.

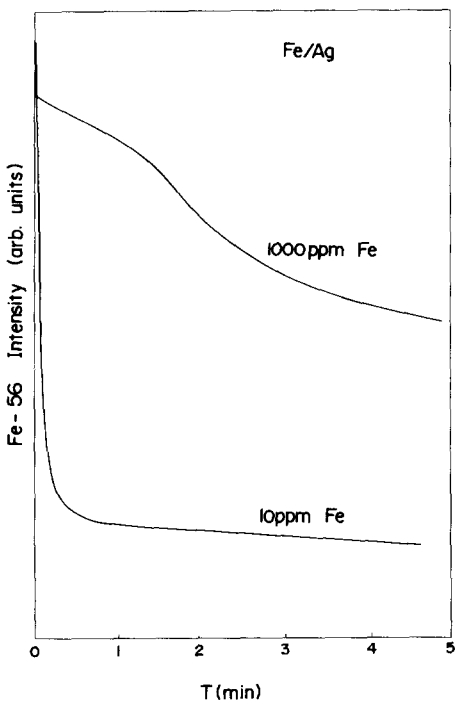

FIG. 6. The depth profile of iron for slightly poisoned catalysts and seriously poisoned catalysts. The primary energy of Ar^+ is 5.5 keV.

FIG. 7. SEM(S-520) micrographs for seriously poisoned catalyst.

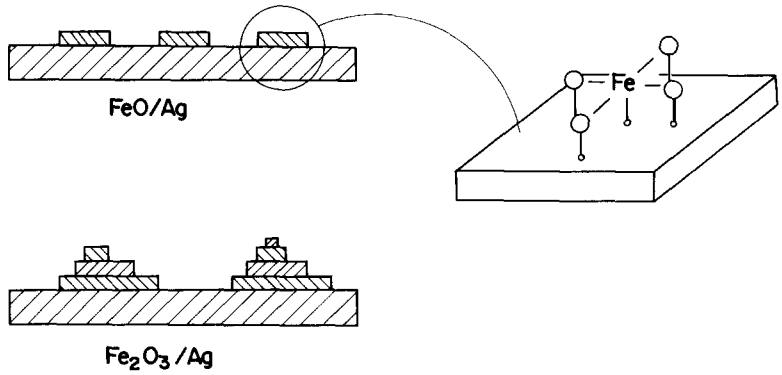

FIG. 8. Schematic representation of surface structure on the slightly (top) and seriously (bottom) poisoned catalysts.

a submonolayer quantity. XPS proved that the iron submonolayer is present as the low oxidation state, FeO. The reason why this species does not further transform to high oxidation states, e.g., Fe_3O_4 and Fe_2O_3, may possibly be explained by analyzing the special structure of FeO on the silver surface. The XPS bonding energy shifts of O(1*s*) and work function change indicate that the Fe(II) cation interacts strongly with the silver atom by oxygen coordination (see Fig. 8). The electrons transfer from the silver 3*d* orbital to the oxygen 2*p* orbital and result in the formation of strong bonding between the silver substrate and the coordinated oxygen. The strong interaction makes a thermally stable FeO species on the surface. In our previous studies (*13*), theoretical analysis shows that the effect of preadsorbed oxygen is to modify the electronic properties of the silver surface. The surface atoms of silver transfer their electrons to oxygen and produce electron deficient sites. The positive site is somewhat like a Lewis acid, which favors adsorption and the reaction of methanol (*1*). It is reasonable to assume that the effect of FeO on the surface is just like that of preadsorbed oxygen on the silver surface. The electron deficient site plays the Lewis acid role on the surface, which favors the adsorption and the reaction of methanol.

When the iron loading is increased until multilayers are formed, the effect of ligand field becomes dominant, which favors agglomeration of iron oxides. The formation of iron islands weakens the interactions of the iron with the silver substrate. On further increasing the iron loading, the interaction disappears, and islands of Fe_2O_3 are found.

4. *The Adsorption and Decomposition of CH_3OD over FeO/Ag*

Figure 9 shows the change of work function for CH_3OD adsorption on the FeO/Ag surface with various methanol exposures at room temperature. The adsorption of CH_3OD leads to the decrease of work function, indicating the electron donation from CH_3OD to the surface. The TDS spectrum of methanol desorption is shown in Fig. 10. These curves were monitored by recording CH_3OD (mass 33). Neither CH_3OH (mass 32) nor CH_3O (mass 31) signals were observed, which implies that on this surface no dissociative adsorption occurs, and the adsorption intermediate is present as a nondissociative species.

Figure 11 is a temperature-programmed decomposition spectrum for CH_3OD adsorption on FeO/Ag surface. The CH_3OD exposure was 460 Langmuir at 300 K. With increasing sample temperature, the adsorption intermediate decomposed via two reaction channels at 380 and 550 K, yielding CH_3OD, CO, HD, and CH_2O, respectively. Careful studies show that each of these

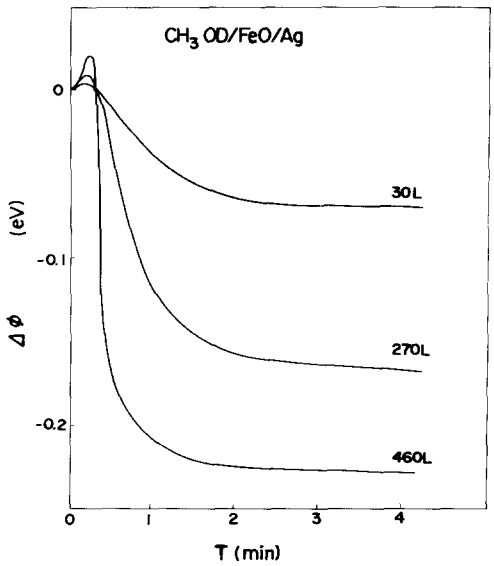

FIG. 9. The change of work function for CH_3OD adsorption on the FeO/Ag surface vs the exposure pressure. (1) 30 L, (2) 270 L, (3) 460 L.

products was formed following first-order kinetics. These observations suggesting the following reaction scheme may be responsible for the decomposition of CH_3OD on FeO/Ag surface.

$$\left.\begin{aligned} &CH_3OD(a) \rightarrow CH_3OD(g) \\ &CH_3OD(a) \rightarrow CO + H_2 + HD \end{aligned}\right\} 380\ K$$

$$\left.\begin{aligned} &CH_3OD(a) \rightarrow CH_3O(a) + D(a) \\ &CH_3O(a) \rightarrow CH_2O(g) + H(a) \\ &H(a) + D(a) \rightarrow HD(g) \end{aligned}\right\} 550\ K$$

The adsorption and reaction of methanol on the clean silver surface has not been observed, but can be observed on the FeO-covered silver surface. This phenomenon is somewhat like the effect of "oxygen-induced adsorption" (*1*).

As is well known, the oxygen in FeO draws electrons from metallic silver and creates electron deficient sites (acts as Lewis acid) on the adjacent surface silver atom. When methanol approaches to the surface, the lone pair of electrons (acts as Lewis base) contained in the oxygen 2*p* orbital interacts directly with the electron deficient sites and forms an adsorption intermediate on the surface. The transmission of surface electron leads to the decrease of work function, which is in agreement with our results. These two types of induced-adsorption processes are depicted for the case of adsorption of methanol in Fig. 12.

5. *The Adsorption of Oxygen on Iron-Covered Silver*

The thermal desorption spectra of oxygen ($^{18}O_2$) from FeO/Ag, Fe_2O_3/Ag, and pure Ag are given in Fig. 13. On the FeO/Ag surface, the desorption peak is centered around 570 K and shifted to lower temperature by about 40 K from that on clean Ag. For O_2 adsorption, the adsorption heat is decreased from 143 kJ/mol on a clean silver to 117 kJ/mol. The weakening of Ag–O bonding can be explained by the presence of strong interaction

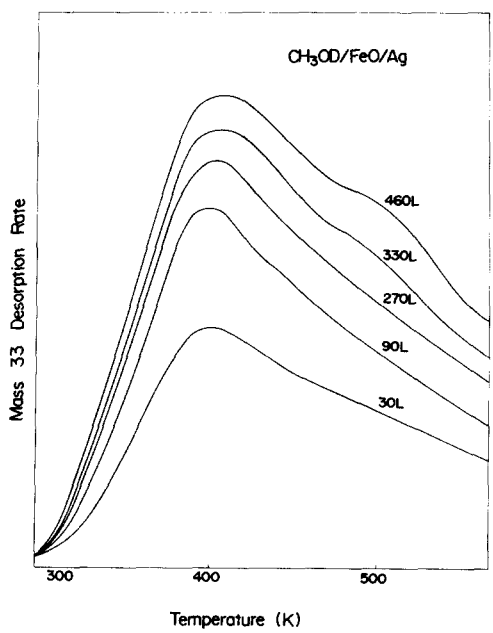

FIG. 10. CH_3OD desorption from FeO/Ag following exposure at room temperature.

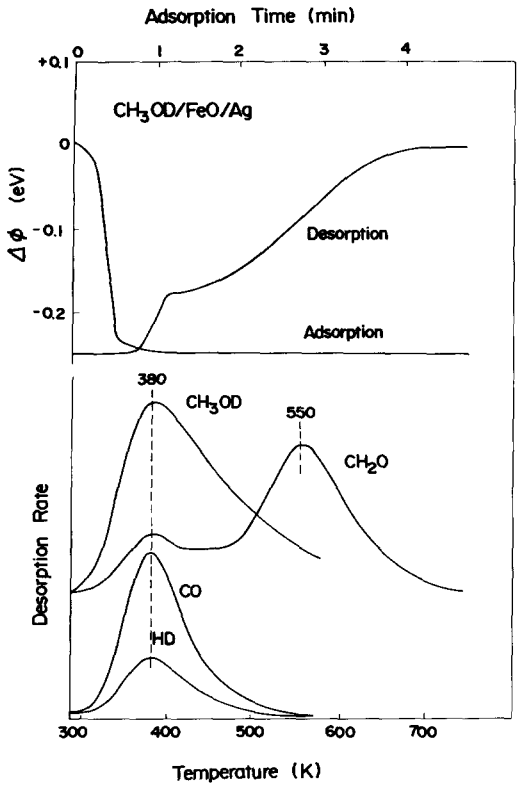

FIG. 11. The work function change (top) and the product distribution (bottom) after exposure of the FeO/Ag surface with CH_3OD of 460 L at room temperature.

of FeO with silver, which would weaken the electron donation ability from a silver atom of adsorbed oxygen. On the Fe_2O_3/Ag surface, the high-temperature peak slightly shifts to higher temperature by about 5K from that on clean Ag. Based upon the desorption kinetic parameters, this peak can be ascribed to the oxygen desorption from iron-free silver sites. The new peak at 480 K is asymmetrical, and the desorption kinetic is first order, with an activation energy 40–50 kJ/mol. The thermal desorption of oxygen on Fe_2O_3 powder has been investigated by Yang and Kung (*15*), and a desorption peak of oxygen centered at about 500 K has been observed. Our previous results have proved that the Fe_2O_3/Ag surface shows a disordered island structure and the independent particles of Fe_2O_3 have been detected. We believe that the new peak is contributed by the desorption of the oxygen adsorbed on the islands of Fe_2O_3.

6. *The Oxidation of Methanol over Iron-Covered Silver*

Steady-state TPRS was used to investigate the reaction behavior of methanol over the iron-covered silver. The condition chosen for testing is as follows: partial pressure of $^{18}O_2$, 1×10^{-7} Torr, partial pressure of methanol, 2×10^{-7} Torr, and the heating rate was 29 K/min. During testing, the dosing rate of both $^{18}O_2$ and methanol were kept constant and the partial pressure of reactants and products were monitored simultaneously.

The product distribution of SSTPRS for methanol oxidation over FeO/Ag and Fe_2O_3/Ag are shown in Figs. 14 and 15, respectively. The data presented in Table 2 are the reaction parameters and the product distributions on Ag (*8*), FeO/Ag, and Fe_2O_3/Ag.

From these results, it is clearly seen that for the pure silver the starting reaction temperature is 400 K, which is shifted to 375 and 350K, and the activation energy calculated by $\ln(T_p^2/\beta)$ versus $1/T_p$ is decreased by about 10 and 20 kJ/mol on FeO/Ag and Fe_2O_3/Ag, respectively. Our previous discussions show that on FeO/Ag surfaces, the electron deficient sites created by surface FeO, which demotes the electron transmission from silver atom to adsorbed oxygen, resulting in the weakening of the adsorbed Ag/O bond. On the Fe_2O_3/Ag surfaces the adsorption of oxygen on the islands of Fe_2O_3 develops a more active oxygen species with E_d = 58 kJ/mol, which bypasses the reaction path of stable methoxide formation and enhances the combustion reaction of methanol.

TABLE 2

The Comparison of Reaction Parameters in Methanol Oxidation over Various Catalysts

Sample	T_{start} (K)	E kJ/mol	Product distribution		
			CH_2O%	CO%	CO_2%
Ag	400	101	50	0	40
FeO/Ag	375	95	0	40	60
Fe_2O_3/Ag	350	85	0	<5	>90

governed by the surface iron species. The oxidation state of iron, as indicated by XPS binding energy shifts of Fe($2p$), increases with the poisoning degree from pure FeO to Fe_3O_4 and finally to Fe_2O_3. Work function experiments confirm that on the surface of low iron-loaded catalyst the Fe(II) cation interacts strongly with the silver atom by means of oxygen coordination, the electrons transfer from silver to oxygen, and a strong bonding is formed between the coordinated oxygen and the substrate. SIMS and SEM results show that further increase in iron coverage gives a multilayer of iron and then islands of Fe_2O_3, which are due to the disappearance of the strong interactions between iron oxides species and silver substrate.

(2) CH_3OD is adsorbed nondissociatively on FeO/Ag surfaces, and the subsequent heating results in decomposition of the adsorbed species. The decomposition follows two reaction channels and yields CH_3OH,

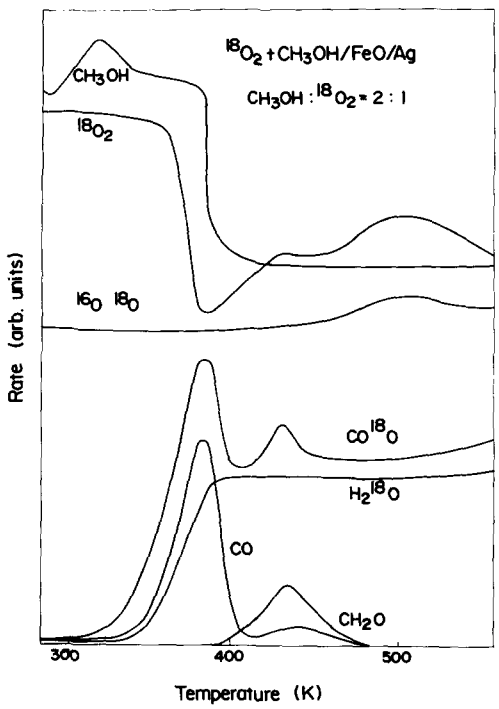

FIG. 14. The products distribution of SSTPRS for methanol oxidation over FeO/Ag surface, oxygen relative to methanol was 0.50.

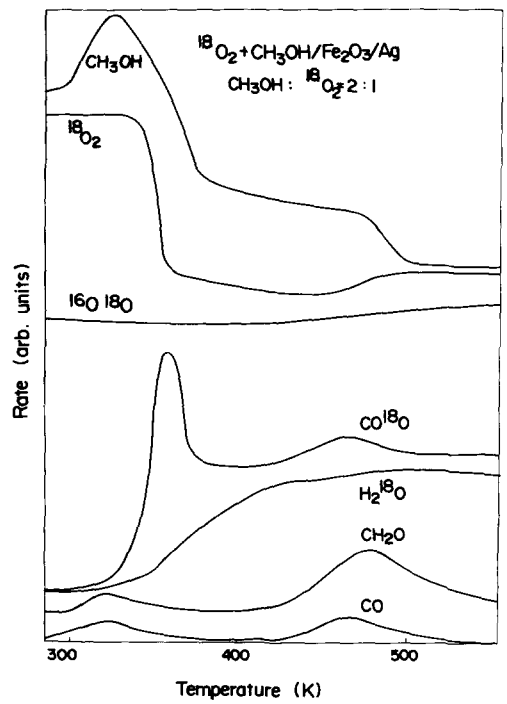

FIG. 15. The products distribution of SSTPRS for methanol oxidation over Fe_2O_3/Ag surface, oxygen relative to methanol was 0.50.

CO, HD, and CH_2O at 380 and 550 K, respectively (see Fig. 11).

(3) FeO on the surface creates electron deficient sites, which demotes the electron donation to adsorbed oxygen and results in the weakening of adsorption bond of oxygen.

(4) Ferric oxides promote the further oxidation of methanol. The starting temperature for reaction is shifted to lower temperature by about 25 K and 50 K, and the activation energy decreases by about 10 and 20 kJ/mol on FeO/Ag and Fe_2O_3/Ag, respectively.

ACKNOWLEDGMENTS

The authors gratefully acknowledge financial support from the National Science Foundation and the State Education Commission of China. The authors also express gratitude to Tang Liang and Liu Dingjiang for their technical assistance.

REFERENCES

1. Barteau, M. A., and Madix, R. J., *in* "Chemical Physics of Solid Surface and Heterogeneous Catalysis" (D. A. King and D. P. Woodruff, Eds.), Vol. 4, p. 100. Elsevier, Amsterdam, 1982.
2. Deng, J. F., *Chin. Petrochem. Technol.* **8,** 463 (1979).
3. Deng, J. F., Xiang, Y. F., Zhang, X. Z. and Gu, J. W., *Chin. Petrochem. Technol.* **9,** 523 (1980).
4. Hughes, R., "Deactivation of Catalysts," p. 84. Academic Press, San Diego, 1984.
5. Jede, R., and Benninghoven, A., *et al., in* Proceedings, 8th International Congress on Catalysis, Berlin, 1984," Vol. 3, p. 521. Dechema, Frankfurt-am-Main, 1984.
6. Jede, R., Manske, E., Ganschow, O., and Benninghoven, A., *J. Vac. Sci. Technol. A* **3,** 1883 (1983).
7. Wachs, I. E., and Madix, R. J., *Surf. Sci.* **76,** 531 (1978).
8. Bao, X. H. and Deng, J. F., *J. Catal.* **99,** 391 (1986).
9. Deng, J. F., Xiang, Y. F., Ye, L. Y., and Zhu, X. Z., *Chin. J. Catal.* **4,** 266 (1983).
10. Dong, S. Z., Bao, X. H. and Deng, J. F., *Acta Phys. Chim. Sin.* **2,** 1 (1986).
11. Bao, X. H., Dong, S. Z., and Deng, J. F., *Surf. Sci.* **163,** 444 (1985).
12. Brundle, C. R., Chuang, T. J., and Wandelt, K., *Surf. Sci.* **68,** 459 (1977).
13. Wandelt, K., *Surf. Sci. Rep.* **2,** 1 (1982).
14. Fan, K. N., Bao, X. H., and Deng, J. F., *Acta Chim. Sin.* **48,** 330 (1990).
15. Yang, B. L., and Kung, H. H., *J. Catal.* **75,** 329 (1982).